# An algorithm for selecting the mass ratio of electrodes in lithium-ion batteries for the fast charging mode

© D.S. Ilyushchenkov, S.A. Gurevich, A.V. Platonov

Ioffe Institute, St. Petersburg, Russia
E-mail: dmitry@mail.ioffe.ru

The paper proposes an algorithm for selecting the optimal mass balance of electrodes of a lithium-ion battery operating in the fast charging mode. The algorithm is based on a numerical model describing the operation of batteries with electrodes produced by using porous materials filled with liquid electrolyte. The calculations employed the data on characteristics of electrode materials, including values of reversible and irreversible capacity determined at low currents. It is shown that this model describes well the behavior of batteries with an NCM622-based cathode and nanocarbon anode even in the mode of fast two-stage high-current charging. Using the model developed, it is possible to determine the ratio of the anode and cathode masses, which is optimal to achieve the maximum specific energy of the battery in any given operating mode, without conducting labor-consuming experiments.

Due to their high energy capacity and power, lithium-ion batteries (LIBs) occupy a special place in modern technology: they are widely used as power sources for portable electronic devices [1], dominate the field of power supplies for electric transport vehicles [2], and are used for energy storage in networks [3]. One of the important problems related to the LIB manufacturing technology is selecting such an optimal ratio between the masses of the anode and cathode active materials that makes the potentials of both electrodes varying during the LIB operation in a preset voltage range. When the optimal mass balance is disturbed, the electrodes get overcharged; this initiates various negative effects, such as electrolyte decomposition, irreversible chemical reactions, and degradation of the electrode active materials, which reduce the battery's capacity and service life.

The task assigned may seem trivial, since the certified capacity and quasi-equilibrium charging/discharging curve are known for each electrode active material. This would seem to be sufficient for simple calculation of the ratio between the anode and cathode masses. However, certified capacities are always measured at ultra-low currents (10 to 20 hours per charging) that do not match the batteries' real operating conditions. As the current increases, the achievable capacity and working voltage window change, the changes at the cathode and anode being different. For instance, the achievable anode-graphite capacity in the case of 30 min charging is more than 3 times lower than that at ultra-low currents. At the same time, cathode materials based on oxides and phosphates lose only tens of percent of their capacity in the 30 min charging mode. Practically, this means that, when the mass balance determined at low currents is used in the fast charging mode, a significant part of the cathode capacity remains unutilized. Thus, the

problem of selecting the optimal balance with accounting for the expected real operating mode of the batteries becomes important. This paper presents an algorithm that allows determining the optimal electrode masses for arbitrary operating modes of batteries based on calculations and experimental data on the electrode material properties. As an example, we have considered the case of ultra-fast charging for the anode made from the material based on amorphous nanostructured carbon ($n$C) created by the authors [4]. Unlike graphite, this material allows for ultra-fast charging and remains stable over thousands of cycles.

In this paper we consider LIBs with anodes based on $n$C and cathodes made of commercially available material NCM622 (NCM). As the electrolyte, a one-molar solution of salt $LiPF_6$ in the 1:1 mixture of ethylene carbonate (EC) and diethyl carbonate (DEC) is used. To determine experimentally the $n$C parameters, cells (in the CR2032 case) with a counter-electrode made of metallic lithium ($n$C/Li) were fabricated. The working electrode was formed from a suspension consisting of $n$C (92 wt.%), conductive carbon black Super C65 (4 wt.%), and binder made of carboxymethylcellulose (1.7 wt.%) and butadiene-styrene rubber (2.3 wt.%). Standard separator Celgard 2325 with the porosity of 39% was used. The cells fabricated were cycled in the galvanostatic mode in the current range of 0.1C to 3C (current 0.1C corresponds to charging/discharging for 10 h, current 3C corresponds to charging/discharging for 20 min). Cycling at low currents allowed us to determine the reversible and irreversible capacities of $n$C, which turned out to be 440 and 40 mA · h/g, respectively. Cycling at high currents made it possible to estimate the cell resistance and working electrode overvoltage. Analysis of the obtained charging/discharging curves has shown the presence of the $n$C potential hysteresis whose description needed determin-
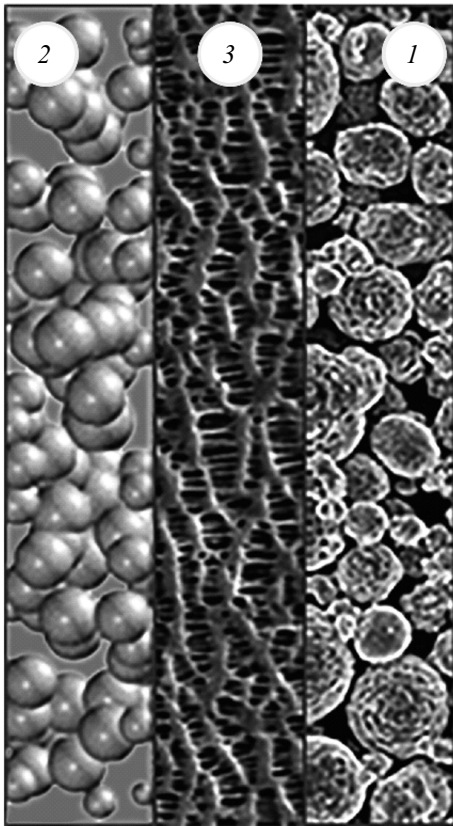
**Figure 1.** Schematic diagram of a lithium-ion battery. *1* — cathode made of porous material NCM622, *2* — anode made of amorphous nanostructured carbon, *3* — separator.



**Figure 2.** Comparison of experimental data (black curves) and numerical calculations (red curves) for three-electrode cell NCM/nC. Time dependence of the cathode potential (with respect to Li/Li$^+$) (*1*), anode potential (*2*), and cell voltage (*3*). The colored figure is given in the electronic version of the article.

ing different values of the effective equilibrium potential for charging and discharging.

The NCM parameters were determined from experiments on galvanostatic cycling of NCM/Li cells (also in the CR2032 case) at the currents ranging from 0.1C to 3C. In this case, the working electrode was formed from a suspension of the following composition: NCM622 — 96 wt.%, conductive carbon black (Super C65) — 2 wt.%, binder (polyvinylidene fluoride) — 2 wt.%. The NCM specific reversible capacity measured at a low current appeared to be 175 mA · h/g, while irreversible capacity was 40 mA · h/g. The obtained parameters of NCM are consistent with its Specifications. Based on the results of high-current cycling, the cell resistance and working electrode overvoltage were determined.

Besides the test cells with the lithium counter electrode, which were used to characterize the materials, full NCM/nC cells were also fabricated. Those cells contained an additional reference lithium electrode located between two separator layers (and covering a small (∼ 10%) portion of the electrode area). Using such a three-electrode cell, we succeeded in measuring not only the voltage between the cathode and anode, but also the potential of each electrode with respect to lithium. The results of experiments on cycling full NCM/nC cells were compared with the results
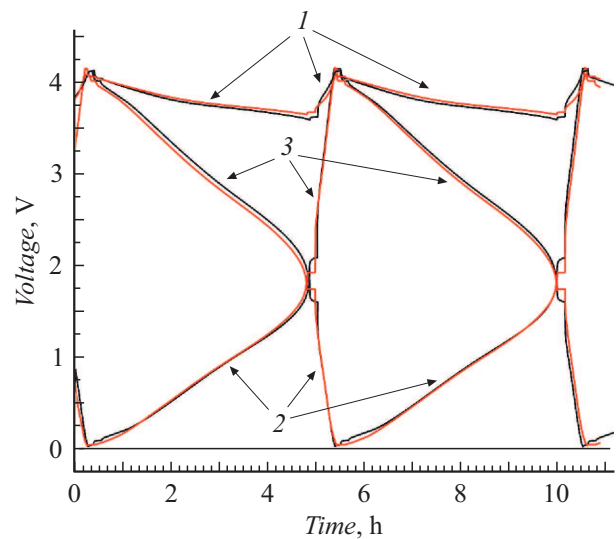
of simulation; this enabled us to evaluate applicability of the used model for describing the LIB operation.

The LIB characteristics were calculated with the pseudo-two-dimensional model within which the battery internal structure is presented in the form of three regions (layers) corresponding to the positive electrode, negative electrode and separator between them (Fig. 1). All the three regions are porous media filled with liquid electrolyte. Active materials of the electrodes are represented as solid spherical micron-sized particles. One of the model dimensions corresponds to the line perpendicular to the battery structure layers; the other (pseudo-dimension) corresponds to the electrode particle radius. The model's fundamental equations include conservation laws for the current density in the electrodes and electrolyte, mass balance of the lithium salt in the electrolyte, and mass balance of lithium ions in the solid particles described by the Fick's law within the framework of limited diffusion. The exchange current density of the electrochemical reaction at the electrode−electrolyte interface is described by the Butler−Volmer kinetic equation. The activation potential accounts for the potential difference between the solid and liquid phases of the porous electrode, equilibrium potential of the electrode active substance, and ohmic losses and overvoltage at the electrode−electrolyte interface. The model similar to that used in our study was described in detail in [5].

In calculations based on the model under consideration, the total capacity of the electrodes was represented as a sum of reversible capacity, irreversible capacity associated with blocking of lithium, and irreversible capacity associated with blocking of free sites in the electrode material available for

**Table 1.** Electrode parameters used in modeling

| Parameter | $n$C | NCM622 |
|---|---|---|
| Equilibrium potential | Experimental data in cycling at 0.1C | Experimental data in cycling at 0.1C |
| Reversible capacity, mA · h/g | 440 | 175 |
| Irreversible capacity, mA · h/g | 40 | 40 |
| Electrode porosity | 0.52 | 0.49 |
| Particle size, $\mu$m | 5.0 | 12.5 |
| Diffusion coefficient, cm$^2$/s | $4 \cdot 10^{-10}$ | $1.5 \cdot 10^{-10}$ |
| Electronic conductivity of the active material, mS/cm | 50 | 1.7 |
| Exchange current, mA/cm$^2$ | 0.2 | 0.2 |
| Transfer coefficient of the anodic process | 0.5 | 0.5 |
| Transfer coefficient of the cathodic process | 0.5 | 0.5 |
| Ohmic resistance at the interface, $\Omega \cdot$ cm$^2$ | 10 | 10 |
| Double layer capacity, $\mu$F/cm$^2$ | 20 | 20 |

**Table 2.** Parameters of electrolyte 1M LiPF$_6$ in EC/DEC (1:1)

| Parameter | Value |
|---|---|
| Diffusion coefficient, cm$^2$/s | $1.4 \cdot 10^{-6}$ |
| Ionic conductivity, mS/cm | 7.9 |
| Cation transference number | 0.16 |
| Activity coefficient | 0.63 |

lithium intercalation. The possibility of both the electrode prelithiation and blocking of a part of its capacity with lithium in the event of insufficient capacity on the opposite electrode was also taken into account. Numerical simulation based on this model was performed with the Comsol Multiphysics® package using the calculated Lithium−Ion Battery interface with the aid of the nonlinear Newton method and linear solver PARDISO.

The algorithm for simulating the LIB operation was as follows. In simulating the operation of full NCM/$n$C cells, it was assumed that in the initial state lithium is concentrated in the cathode material NCM. Then the preset mode of cell cycling was started, during which stages of direct current flow (charging or discharging) in the given voltage range and pauses in the modes of dc voltage or open circuit were periodically repeated.

Fig. 2 presents, as an example of applying the considered model, the experimental and calculated dependences of the anode and cathode potentials and total cell voltage obtained during galvanostatic cycling of the three-electrode NCM/$n$C cell. In this example, the ratio between masses of the cathode and anode active materials was $m_{NCM}/m_{nC} = 3.6$. Cycling was performed in the following order: charging at the direct current of 2C, subsequent additional charging at the dc voltage of 4.2 V until the current drops to 0.2C, and discharging at the current of 0.2C to the voltage of 1.8 V with 15 min intervals between charging and discharging. The main parameters of the electrode material and electrolyte used in the numerical simulation are given in Tables 1 and 2, respectively. It is evident that the model developed describes well the battery behavior during discharging and charging, despite the complexity of the two-stage charging mode.

Fig. 3 presents the numerically simulated dependences of the NCM/$n$C battery specific energy during charging and discharging on the ratio between masses of the anode and cathode active materials. The charging/discharging mode was as follows: charging at the direct current of 4C, subsequent additional charging at the dc voltage of 4.2 V until the current drops to 1C, holding in the idle mode for 10 min, and then discharging at the current of 0.2C to the voltage of 1.8 V with 10 min holding in the idle mode. Such a mode may be relevant for ultra-fast charging of the electric vehicle batteries. The dependences presented in Fig. 3 demonstrate the existence of an optimal ratio between the anode and cathode masses, at which the maximum specific energy of the battery gets achieved; this was later confirmed experimentally in cycling cells with different ratios of electrode masses. Note that the ratio of discharging and charging energies shown in Fig. 3 has the meaning of the battery efficiency in this mode. It is evident that the efficiency is close to 90 % in the entire range of the mass ratios.

Note in conclusion that the use of the proposed algorithm for determining the optimal ratio of electrode masses for the given battery charging/discharging mode allows one to avoid performing a large number of labor-consuming experiments, which is especially important in the case of using active
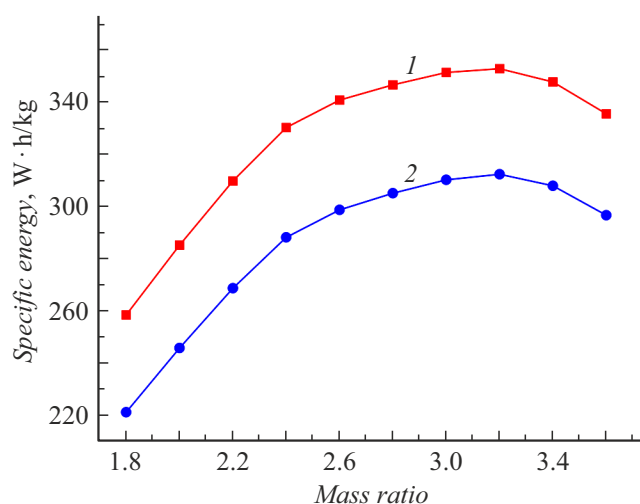
**Figure 3.** Results of numerical calculation of the specific energy density dependences on the ratio of the electrode masses during charging (*1*) and discharging (*2*) of the NCM/*n*C cell (the charging/discharging mode is described in the text).

materials like amorphous nanostructured carbon allowing operation at high currents.

## Funding

## Conflict of interests

The authors declare that have no conflict of interests.

## References

[1] Y. Liang, C.-Z. Zhao, H. Yuan, Y. Chen, W. Zhang, J.-Q. Huang, D. Yu, Y. Liu, M.-M. Titirici, Y.-L. Chueh, H. Yu, Q. Zhang, InfoMat, **1** (1), 6 (2019). DOI: 10.1002/inf2.12000

[2] A. Masias, J. Marcicki, W.A. Paxton, ACS Energy Lett., **6** (2), 621 (2021). DOI: 10.1021/acsenergylett.0c02584

[3] A.A. Kebede, T. Kalogiannis, J.V. Mierlo, M. Berecibar, Renew. Sustain. Energy Rev., **159**, 112213 (2022). DOI: 10.1016/j.rser.2022.112213

[4] S. Ahn, M. Lagnoni, Y. Yuan, A. Ogarev, E. Vavrinyuk, G. Voynov, E. Barrett, A. Pelli, A. Atrashchenko, A. Platonov, S. Gurevich, M. Gorokhov, D. Rupasov, A.W. Robertson, R.A. House, L.R. Johnson, A. Bertei, D.V. Chernyshov, ACS Appl. Energy Mater., **6** (16), 8455 (2023). DOI: 10.1021/acsaem.3c01280

[5] Y. Li, K. Li, W. Shen, J. Huang, X. Qu, Y. Zhang, Y. Lin, J. Energy Storage, **86** (A), 111165 (2024). DOI: 10.1016/j.est.2024.111165

*Translated by EgoTranslating*